A Resolution Function Model For A Multi-Analyser Spectrometer

M.Hagen[1,2] and U.Steigenberger[1]

[1]ISIS Facility, Rutherford Appleton Laboratory, Didcot, Oxon. OX11 0QX, U.K.
[2]Department of Physics, Keele University, Keele, Staffs. ST5 5BG, U.K.

Abstract
We have formulated a mathematical description of the resolution function for a multi-analyser spectrometer at a pulsed source. This formulation has been tested by a comparison with measurements carried out on the PRISMA multi-analyser spectrometer at ISIS. Previous theoretical formulations of the resolution function for multi-analyser spectrometers have assumed that that the asymmetry of the incident neutron pulse from the source could be ignored. Our measurements have shown that this is not the case for PRISMA and our formulation is such that this asymmetry has been taken into account.

1 Introduction

The technique of inelastic neutron scattering is unrivalled in its ability to measure phonon and spin wave dispersion relations and these measurements provide invaluable information on the inter-atomic forces in a solid. The anisotropic nature of a crystal structure means that dispersion relations can be very different in different reciprocal lattice directions and that such measurements must be carried out using single crystal samples. At reactor neutron sources this type of measurement has been carried out using the triple axis spectrometer which was devised by Brockhouse in the 1950's [1], while at spallation sources they have been carried out by multi-analyser spectrometers such as MAX [2] and PRISMA [3]. The lineshape of phonons measured on all of these instruments is given by the convolution integral of the spectrometer resolution function with the dynamic structure factor for the phonon dispersion surface. The resolution function is the relative probability of observing a neutron scattered with a wavevector and energy transfer $(\mathbf{Q}_0 + \Delta\mathbf{Q}, E_0 + \Delta E)$ when the spectrometer was positioned to measure $(\mathbf{Q}_0, E_0)$. It reflects the probability of transmission/reflection of a neutron through the various beam defining elements of the spectrometer with a wavevector or divergence other than the

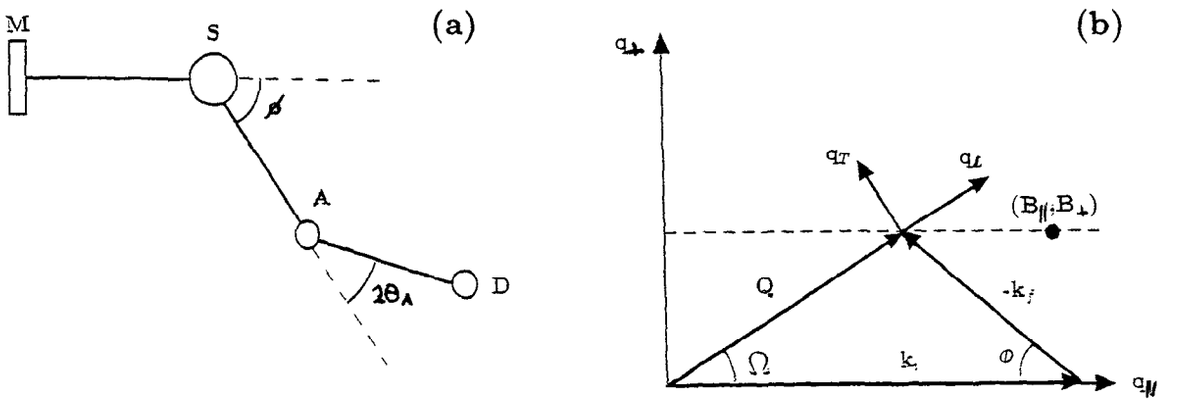

Figure 1: (a) A schematic diagram of a single analyser-detector system on a multi-analyser spectrometer is shown. (b) The path followed in reciprocal space in an indirect geometry inelastic scattering measurement is shown by the dashed line.

nominal values.

A model for the resolution function of the triple axis spectrometer was produced some time ago by Cooper and Nathans [4] in which all of the spectrometer elements are treated as having Gaussian probability distributions for their transmission/reflection elements. The combination of these elements, subject to the scattering conditions at the monochromator, sample and analyser, leads to a four dimensional Gaussian resolution function in $(\Delta\mathbf{Q}, \Delta E)$. However at a spallation source there is an intrinsically non-Gaussian component in the formulation of the resolution function, the initial neutron pulse shape in time of flight. In this paper we briefly review a recent formulation of the resolution function for a multi-analyser spectrometer which takes account of this non-Gaussian component. A detailed derivation has been given elesewhere [5].

2 Resolution Function Formalism

A multi-analyser spectrometer, such as MAX or PRISMA, has a bank of analyser-detector systems [2, 3]. However for the purposes of formulating the resolution function we need only consider a single analyser-detector set-up. In figure 1a a schematic representation of this single analyser-detector system is shown where M is the moderator, S is the sample, A is the analyser and D the detector. Inelastic measurements are carried out using the indirect geometry technique in which the analyser crystal defines the final wavevector and

the time of flight measurement is used to scan the incident wavevector. The wavevector transfer in the inelastic measurement, $\mathbf{Q} = \mathbf{k}_i - \mathbf{k}_f$, is therefore scanned along a path parallel to $\mathbf{k}_i$. In figure 1b we show schematically by the dashed line the path followed in such a measurement. The wavevector can be written in terms of components parallel to, and perpendicular to $\mathbf{k}_i$ as $\mathbf{Q} = Q_{\|}\hat{\boldsymbol{q}}_{\|} + Q_{\perp}\hat{\boldsymbol{q}}_{\perp}$. Along this path the energy transfer of the neutron varies as $E = (\hbar^2/2m_N)(k_i^2 - k_f^2) = (\hbar^2/2m_N)(Q_{\|}^2 + 2(Q_{\perp}\cot\phi)Q_{\|} - Q_{\perp}^2)$.

The resolution function for the system shown in figure 1a can be therefore be written as an integral over the various paths through the different spectrometer elements weighted by their probability distributions for transmission/reflection in the form ;

$$\begin{aligned} R(\mathbf{Q},E) \;=\; & \int d\gamma_1\, d\gamma_2\, d\gamma_3\, d\varepsilon_1\, d\varepsilon_2\, d\varepsilon_3\, d\eta_{HS}\, d\eta_{VS}\, d\eta_{HA}\, d\eta_{VA}\, dk_i\, dk_f\, dk_f'\, dT_0 \;\times \\ & P_{H1}(\gamma_1)\, P_{H2}(\gamma_2)\, P_{H3}(\gamma_3)\, P_{V1}(\varepsilon_1)\, P_{V2}(\varepsilon_2)\, P_{V3}(\varepsilon_3)\, P_{HS}(\eta_{HS}) \;\times \\ & P_{HA}(\eta_{HA})\, P_{VS}(\eta_{VS})\, P_{VA}(\eta_{VA})\, P(T_0)\, \delta(T - T_0 - T_i - T_f) \;\times \\ & \delta((\mathbf{Q} - \eta_{HS}Q_0\hat{\mathbf{Q}}_T - \eta_{VS}Q_0\hat{\mathbf{Q}}_V) - \mathbf{k}_i + \mathbf{k}_f)\, \delta(E - \frac{\hbar^2}{2m}(k_i^2 - k_f^2)) \;\times \\ & \delta((\boldsymbol{\tau}_A - \eta_{HA}\tau_A\hat{\boldsymbol{\tau}}_T - \eta_{VA}\tau_A\hat{\boldsymbol{\tau}}_V) - \mathbf{k}_f + \mathbf{k}_f')\, \delta(k_f - k_f') \end{aligned} \qquad (1)$$

The angles γ_i and ε_i $(i = 1,2,3)$ are the horizontal and vertical divergences of the beam from the nominal moderator to sample, sample to analyser and analyser to detector directions respectively and $P_{Hi}(\gamma_i)$ and $P_{Vi}(\varepsilon_i)$ the corresponding collimator transmission functions. The angles η_{AB} ($A = H,V$, $B = S,A$) are the horizontal and vertical mosaic spreads and $P_{AB}(\eta_{AB})$ the mosaic spread distribution functions for the sample and analyser crystals respectively. The function $P(T_0)$ is the initial pulse shape in time of flight. The first delta-function in equation(1) accounts for the time of flight of the neutrons, T is the arrival time at the detector, T_0 is the time at which the neutrons leave the moderator and T_i and T_f are the flight times from moderator to sample and sample to detector respectively. The second and third delta functions account for the conservation of wavevector and energy transfer at the sample. The wavevector has been modified to account for the sample mosaic using the Werner and Pynn approximation [6] where $\hat{\mathbf{Q}}_T$ and $\hat{\mathbf{Q}}_V$ are unit vectors perpendicular to $\mathbf{Q}_0$ in the horizontal and vertical planes. The fourth and fifth delta functions enforce the Bragg scattering condition at the analyser, where $\boldsymbol{\tau}_A$ is the scattering vector of the analyser planes. The wavevectors $\mathbf{k}_f$ and $\mathbf{k}_f'$ are the neutron wavevectors as scattered from sample to analyser and from analyser to detector. The mosaic spread of the analyser has been included in a similar fashion to that for the sample.

If all of the P-functions in equation(1) are modelled by Gaussians except for $P(T_0)$ and all of the integrals then performed, with the exception of the integral over T_0, then the result is ;

$$R(\mathbf{Q},E) = R_0 \exp\left[-\frac{1}{2}\left(\left(\frac{\Delta Q_V}{\sigma_V}\right)^2 + \tilde{x}^T\tilde{M}\tilde{x}\right)\right] \int dT_0\, P(T_0) \exp\left[-\frac{1}{2}\left(\frac{T_0 - \tilde{t}^T\tilde{x}}{\sigma_T}\right)^2\right] \qquad (2)$$

where $\tilde{x} = \left[\Delta Q_{||}, \Delta Q_{\perp}, \Delta E\right]$ and ΔQ_V is the vertical component. The matrix elements of $\tilde{M}$ and $\tilde{t}$ and the expressions for σ_V and σ_T are given in ref. [5]. As in the case of the triple axis resolution function [4] the terms in ΔQ_V separate out from those in $\Delta Q_{||}, \Delta Q_{\perp}$ and ΔE.

Equation(2) is a general result for any pulse shape $P(T_0)$ and in order to assess the practical importance of the effect of asymmetry in the resolution function we have also considered the specific case of using the simplest asymmetric form $P(T_0) = \Theta(T_0) \exp(-T_0/\tau)$. The result is ;

$$R_H(\mathbf{Q}, E) = R_K \exp\left(-\frac{1}{2}\tilde{x}^T \tilde{M} \tilde{x} - \frac{1}{\tau}\tilde{t}^T \tilde{x}\right) \operatorname{erfc}\left(\frac{1}{\sqrt{2}}\left[\frac{\sigma_T}{\tau} - \frac{1}{\sigma_T}\tilde{t}^T \tilde{x}\right]\right) \tag{3}$$

where the vertical terms, which remain unchanged from equation(2), have been omitted. In this result the slowing down time τ is energy dependent. An empirical form for this energy dependence, relevant to the PRISMA beamline, has been found from Bragg peak and powder diffraction measurements to be [5] ;

$$\tau(E) = \begin{cases} \tau_0 & E < E_c \\ \tau_0 / \left(1 + (E - E_c)^2 / \Gamma^2\right) & E > E_c \end{cases} \tag{4}$$

with the best fit values of $\tau_0 = 37.15$ μsecs, $E_c = 9.0$ meV and $\Gamma = 39.16$ meV. Equation(3) therefore provides a suitable empirical representation of the resolution function of the PRISMA multi-analyser spectrometer from which the effects of asymmetry can be assessed.

3 Discussion

In ref. [5] Bragg peak lineshapes for various crystals and neutron energies were measured and calculated to test equation(3). There was good agreement in all cases and all showed a significant asymmetry. A Bragg peak is probably the case where asymmetry in the resolution function will be most obvious in the measured spectra. In figure (9) of ref. [5] the spectrum measured from a Cu(220) Bragg peak with $E_f = 30$ meV was shown and which had a clearly asymmetric lineshape. In figure 2a we show a contour map of the resolution function in the $Q_{||}, E$ plane relevant to this measurement. Also shown in this figure by the dashed line is the measuring trajectory. Since a Bragg peak is a δ-function in $\mathbf{Q}$ and E the calculated lineshape is essentially given by the intersection of this trajectory (dashed line) with the resolution function. In figures 2b and 2c contour maps of the resolution function in the $Q_{\perp}, E$ and $Q_{||}, Q_{\perp}$ planes are also shown for this particular spectrometer configuration. The effects of asymmetry in the first of these two planes is considerably less marked than in the $Q_{||}, E$ plane. Finally figure 2d shows a contour map of the projection of the resolution function onto the $Q_{||}, E$ plane (ie. the result after integrating over $Q_{\perp}$). This latter form might be appropriate to the situation of phonons in the middle of the Brillouin zone where to a reasonable approximation it might be possible in certain cases to consider the dispersion surface as flat perpendicular

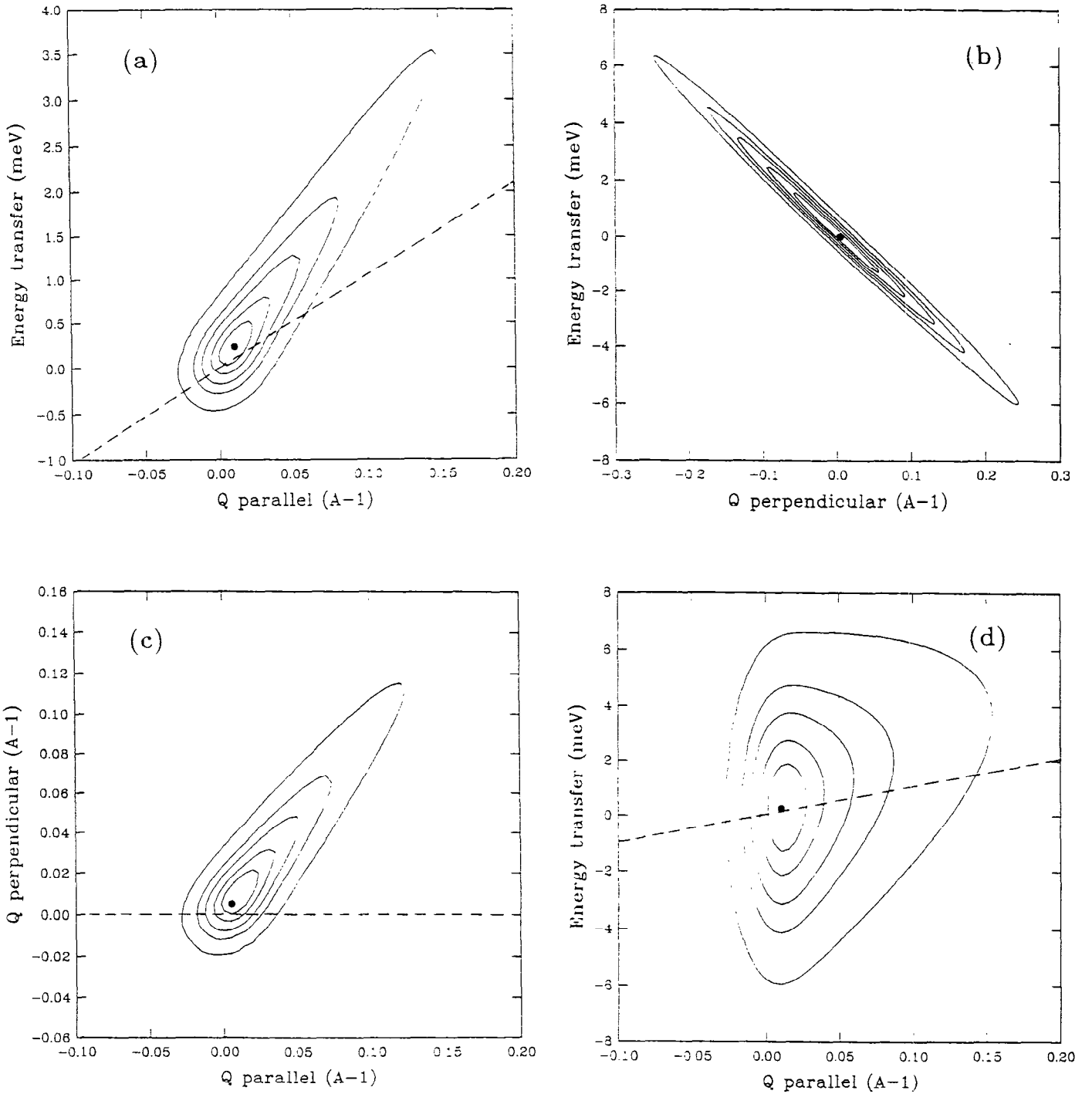

Figure 2: Contour maps of the resolution function for the measurement of a Cu(220) Bragg peak with $E_f = 30$ meV (as discussed in the text) are shown (a) in the $Q_{||}, E$ plane, (b) in the $Q_{\perp}, E$ plane, (c) in the $Q_{||}, Q_{\perp}$ plane and (d) as a projection onto the $Q_{||}, E$ plane. The levels plotted are the 75, 50, 25, 10 and 1 percent levels of the resolution function. The position of the maximum of the resolution function is shown by the dots in (a) to (d) and in (a), (c) and (d) the dashed lines show the path of the measuring trajectory.

to the measuring direction. It is clear that figure 2d is markedly different to that of figure 2a but that although the aymmetry is less marked it is still present. A conclusion that can immediately be drawn from figures 2a to d is that the measured lineshape in an experiment will depend on a detailed consideration of how the dynamic structure factor interacts with the resolution function. It is certainly not possible to replace the resolution function with a simple one dimensional function in energy and then to expect to get the correct results when convoluting with experimental data.

4 Conclusion

A resolution function model for the PRISMA multi-analyser spectrometer has been developed. It has been argued that the measurement of Bragg peaks given in ref. [5] has provided a critical test of the accuracy of including the asymmetry of the pulse shape into the resolution function. The complexity of the resolution function has also been demonstrated and it has been argued that it cannot simply be treated as a one dimensional function in energy only.

References

[1] B.N.Brockhouse, in: Inelastic Scattering of Neutrons in Solids and Liquids (IAEA, Vienna,1961) p. 113

[2] K.Tajima, Y.Ishikawa, K.Kanai, C.G.Windsor and S.Tomiyoshi, Nucl. Instr. and Meth. **201** (1982) 491

[3] U.Steigenberger, M.Hagen, R.Caciuffo, C.Petrillo, F.Cilloco and F.Sachetti, Nucl. Instr. and Meth. **B 53** (1991) 87

[4] M.J.Cooper and R.Nathans, Acta Cryst. **23** (1967) 357

[5] M.Hagen and U.Steigenberger, Nucl. Inst. and Meth. **B 72**, 239 (1992)

[6] S.A.Werner and R.Pynn, J.Appl.Phys. **42** (1971) 4736